



**HAL**  
open science

## Quantum Coherence Preservation in Extremely Dispersive Plasmonic Media

Yury S Tokpanov, James S Fakonas, Benjamin Vest, Harry A Atwater

► **To cite this version:**

Yury S Tokpanov, James S Fakonas, Benjamin Vest, Harry A Atwater. Quantum Coherence Preservation in Extremely Dispersive Plasmonic Media. *Physical Review Applied*, 2019, 12 (4), pp.044037. 10.1103/physrevapplied.12.044037 . hal-04457586

**HAL Id: hal-04457586**

**<https://hal.science/hal-04457586v1>**

Submitted on 14 Feb 2024

**HAL** is a multi-disciplinary open access archive for the deposit and dissemination of scientific research documents, whether they are published or not. The documents may come from teaching and research institutions in France or abroad, or from public or private research centers.


L'archive ouverte pluridisciplinaire **HAL**, est destinée au dépôt et à la diffusion de documents scientifiques de niveau recherche, publiés ou non, émanant des établissements d'enseignement et de recherche français ou étrangers, des laboratoires publics ou privés.

Copyright

## Quantum Coherence Preservation in Extremely Dispersive Plasmonic Media

Yury S. Tokpanov, James S. Fakonas, Benjamin Vest, and Harry A. Atwater<sup>1</sup>\*

*Thomas J. Watson Laboratories of Applied Physics, California Institute of Technology, Pasadena, California 91125, USA*

 (Received 1 May 2019; revised manuscript received 23 June 2019; published 16 October 2019)

Quantum plasmonics experiments have on multiple occasions resulted in the observation of quantum coherence of discrete plasmons, which exhibit remarkable preservation of quantum interference visibility, a seemingly surprising feature for systems mixing light and matter with high Ohmic losses during propagation. However, most experiments to date used essentially weakly confined plasmons, which experience limited light-matter hybridization, thus limiting the potential for decoherence. In this paper, we investigate experimentally the robustness of coherence preservation in a plasmonic system: our setup is based on a hole-array chip supporting plasmons near the surface plasma frequency, where plasmonic dispersion and confinement are much stronger than in previous experiments, making the plasmons much more susceptible for decoherence processes. We, however, report preservation of quantum coherence even in these extreme conditions. We generate polarization-entangled pairs of photons using type-I spontaneous parametric down-conversion and transmit one of the photons through a plasmonic hole array that is numerically designed to convert incident single photons into highly dispersive single surface-plasmon polaritons. Our results show that the quality of photon entanglement after the plasmonic channel is unperturbed by the introduction of a highly dispersive plasmonic element. Our findings provide a lower bound of 100 fs for the pure dephasing time for dispersive plasmons in gold, and show that even in a highly dispersive regime surface plasmons preserve quantum mechanical correlations, making possible harnessing of the power of extreme light confinement for integrated quantum photonics.

DOI: [10.1103/PhysRevApplied.12.044037](https://doi.org/10.1103/PhysRevApplied.12.044037)

### I. INTRODUCTION

Understanding the quantum nature of light and matter is of central importance for advancing modern technology. For example, one approach to physical realization of a quantum computer is envisioned to be through the use of linear optical components [1], which can be arranged in the form of integrated photonic circuits. Since some of the building-block elements for such a scalable quantum photonic system (phase shifters, modulators, directional couplers, etc.) and the coherence and fabrication requirements are very similar to those of present-day chip-based nanophotonic circuit elements, recent experimental advances [2] have inspired optimism about the technical feasibility of quantum integrated photonic systems if suitable single-photon sources, memories, and detectors can be realized.

One of the important branches of photonics is plasmonics, which enables extreme light confinement by using surface-plasmon polaritons (SPPs), the quanta of so-called surface plasma waves that are excited on the boundary between a metal and a dielectric [3]. SPPs are bosons, so their quantum statistical behavior is expected to be

similar to that of photons. By confining electromagnetic energy in small modal volumes, plasmonics allows significantly enhanced light-matter interactions at the nanoscale, and has found interesting applications in classical photonics for sensing [4–6], subdiffraction-limit imaging [7,8], and paving the way toward strong light-matter interactions, by reaching, for example, strong coupling regimes [9,10]. However, light-matter hybridization in SPPs has an important consequence. SPPs are collective excitations of electrons with a mixed electronic and electromagnetic character, while photons in free space are purely electromagnetic excitations, and light propagating through dielectric linear media is described by polaritons, mixing electromagnetic excitation and the motion of bound electrons that do not experience many interactions with the rest of the environment. Through the motion of free electrons in the metal, SPPs are coupled to matter by many degrees of freedom. One consequence is that SPPs experience propagating losses due to the Ohmic losses of the moving electrons composing a SPP. In a fully quantum optical picture, light-matter hybridization could be anticipated to make SPPs sensitive to decoherence from dephasing, which is often present in systems with Ohmic losses, leading to disappearance of their quantum features, such as entanglement.

\*[haa@caltech.edu](mailto:haa@caltech.edu)

Recently, several groups have performed plasmonic analogs to landmark quantum optics experiments using SPPs in lieu of single photons, obtaining results such as the observation of single-plasmons interferences [11,12], of the plasmonic Hong-Ou-Mandel effect [13–15], and of entanglement [16–18]. These successful experiments faced significant plasmonic absorption, manifested as Ohmic losses, but managed to preserve enough of the plasmons to highlight various quantum features of discrete SPPs. However, an apparently surprising result was that most of the experiments performed reported very good or excellent preservation of the quantum interference contrast, possibly indicating that pure dephasing processes are much slower than pure absorption. Notably in each of these experiments, although that the experimental conditions preselected and tested the coherence of the “surviving” nonabsorbed plasmons, the strong plasmonic absorption observed is the undeniable sign of non-negligible coupling between the particles and their environment. The observation of such coupling is an indication that the degrees of freedom of the plasmons are likely to become entangled with the degrees of freedom of the environment, a description that is commonly used to explain the vanishing of quantum interference features, or in other words, decoherence. This has been verified, for example, in an experiment based on plasmonic waveguides [19]. Decoherence is one of the limiting factors for current and future quantum technology. Hence, the question of how SPPs lose quantum mechanical coherence and if their quantum properties can be protected over long propagation distances or under strong light-matter interactions is of significant importance.

Until now, quantum plasmonics experiments used exclusively plasmons in a regime far from the surface plasma frequency. In other words, the plasmons exhibited a highly “photonlike” behavior with weak confinement, which intrinsically limits the decoherence processes. Indeed, in the case of “photonlike” plasmons, we expect the plasmon resonances to have only a weak admixture with the electronic degrees of freedom in the metal, leaving the gateway ajar only to significant coupling and entanglement between the SPPs and the metallic environment. Therefore, in this “photonlike” regime, one could argue that from the perspective of decoherence processes, some quantum plasmonics experiments are somewhat analogous to other quantum optics experiments performed with photons all the way from the source to the detector and exhibiting no decoherence. That would also mean that plasmonic losses here play a role that is not different from optical losses introduced by beam splitters, stray reflections, or neutral-density filters. Thus, there is need to investigate quantum plasmonics in other regimes of plasmon propagation, where the competition between absorption and pure dephasing could result in observable decoherence.

In this paper, we report results of a quantum plasmonics experiment to investigate the robustness of coherence in a highly dispersive plasmon regime and the disappearance of quantum entanglement. More precisely, in a series of experiments inspired by Ref. [16], we measure the preservation of polarization entanglement between two photons after one photon is converted into a plasmon propagating on a hole array, which is then subsequently reconverted into a photon [20–22]. We perform polarization-entanglement experiments in plasmonic hole arrays with circular holes that are designed to be in a highly dispersive regime, (i.e., with single-plasmon energy close to the surface plasma frequency). In this highly dispersive regime, SPPs are tightly confined and have a much stronger interaction with the electronic system (one manifestation of which is significantly greater absorption), which in principle can lead to the destruction of quantum correlations. This experiment aims to build a better understanding of the robustness of quantum phenomena in quantum plasmonics.

## II. RESULTS AND DISCUSSION

In our experimental work, we generate pairs of polarization-entangled photons, propagating along two different paths, and interpose a plasmonic hole array in the path of one of the photons. This photon is thus converted into a plasmon, and the detected signal consists of plasmons reconverted into free-space photons after plasmon propagation over a few hundred nanometers in the hole array [16]. The quality of polarization entanglement between both outcoupled photons is measured and is representative of the effects of light-matter interactions during plasmon propagation. Whereas the work reported in [16] probed hole arrays with linear dispersion (close to light line), we use a plasmonic hole array that operates in a highly dispersive regime (close to the surface plasma frequency) to probe plasmon decoherence. We measure preservation of entanglement between photons even in this regime.

### A. Generation of entangled pairs of particles

As a source of polarization-entangled photons we use type-I spontaneous parametric down-conversion (SPDC) occurring in a pair of nonlinear bismuth borate crystals. They are rotated by  $90^\circ$  with respect to each other and glued together [23] (Fig. 1) so that one crystal has its axis in the horizontal plane and the other has its axis in the vertical plane. The pair of crystals are pumped by a laser diode emitting at 406 nm. The pump photons are linearly polarized at  $45^\circ$  with respect to the nonlinear-crystal axis planes, so type-I SPDC generates pairs of photons at 812 nm that are polarized parallel to either the horizontal direction or the vertical direction with equal probabilities. This setup generates polarization-entangled photons that, before their interaction with the environment  $|E\rangle$  (plasmonic sample),

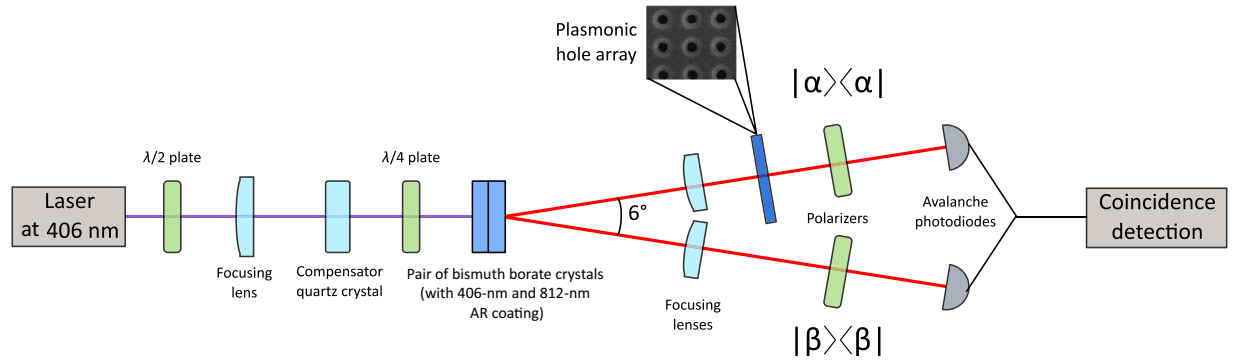


FIG. 1. Experimental setup for the measurement of polarization-entanglement preservation. Pump photons at 406 nm are sent toward a pair of bismuth borate crystals and generate pairs of polarization-entangled photons that propagate along two separate paths. Along the upper path, we can insert a metallic hole array, and we measure the transmission of the entangled light that has been coupled to plasmons. AR, antireflection.

can be described by the superposition state:

$$|\psi\rangle_{\text{initial}} = \frac{1}{\sqrt{2}}[|H, H\rangle + e^{i\Delta\phi_c} |V, V\rangle] \otimes |E\rangle, \quad (1)$$

where  $\Delta\phi_c$  is a phase delay between the two polarizations, due to the birefringence of bismuth borate crystals.

The twin photons propagate in a horizontal plane, along the opposite edges of a cone whose apex angle is  $6^\circ$ . Each photon is focused toward a polarizer and a single-photon avalanche diode. The detection of a photon by one of the single-photon avalanche diodes is a projective measurement of its polarization state. A plasmonic hole array can be placed along one of the propagation paths, thus forcing one of the photons to be temporarily converted into a plasmon before eventually being detected.

In our experiment, to correctly estimate the influence of pure dephasing processes, we retain only coincident counts between the two single-photon avalanche diodes (i.e., we consider only the case when both photons are registered as counts at the detectors). In other words, when the hole array is in place, we do not record events in which a plasmon has decayed through inelastic interactions with the electronic system—this is a well-understood

mechanism for decoherence. On the contrary, we collect photons only from events in which the plasmon has survived. Such events, in principle, can be affected by elastic interactions or the inner structure of the plasmon quasiparticle.

In the general case, after propagation of the quantum entangled state and before applying any projective measurement, we can consider that the light has become entangled with the environment, and we can write

$$|\psi\rangle_{\text{final}} = \frac{1}{\sqrt{|h|^2 + |v|^2}} [h |H, H\rangle \otimes |E_H\rangle + v e^{i\Delta\phi_c} |V, V\rangle \otimes |E_V\rangle], \quad (2)$$

where  $h$  and  $v$  are complex-amplitude transmission coefficients for horizontal polarization  $|H\rangle$  and vertical polarization  $|V\rangle$ , respectively, and  $|E_H\rangle$  and  $|E_V\rangle$  are environmental states, entangled with horizontal and vertical polarization, respectively.

By tracing over environmental states, one can obtain a reduced density matrix, from which the probability of a coincidence count can be computed:

$$P_{\text{CC}}(\alpha, \beta) = \langle \alpha, \beta | \hat{\rho}_{\text{reduced}} | \alpha, \beta \rangle = \frac{1}{1 + \frac{|v|^2}{|h|^2}} \left[ \sin^2 \alpha \sin^2 \beta + \frac{|v|^2}{|h|^2} \cos^2 \alpha \cos^2 \beta + \frac{1}{2} \sin 2\alpha \sin 2\beta \frac{|v|}{|h|} |\langle E_V | E_H \rangle| \cos(\Delta\phi_E + \Delta\phi + \Delta\phi_c) \right], \quad (3)$$

where  $\alpha$  and  $\beta$  are polarizer directions with respect to the vertical axis (see Fig. 1),  $v/h = (|v|/|h|)e^{i\Delta\phi}$ ,  $\Delta\phi$  being the phase difference between the complex amplitudes  $v$  and  $h$ , and  $\langle E_V | E_H \rangle = |\langle E_V | E_H \rangle| e^{i\Delta\phi_E}$ ,  $\phi_E$

being the phase difference between the two environmental states.

The first two terms can be obtained by classical analysis, whereas the last term is the so-called quantum interference

term, which represents the quantum mechanical nature of our system. Indeed, Eq. (2) describes a superposition state. The quantum interference term can be understood as the interference amplitude between the two terms of the superposition state when projective measurements are performed on the two-particle state. The amplitude of this term depends on several factors. It depends sinusoidally on the polarizer directions, and is maximum for appropriate choices of the polarizer directions, verifying  $|\sin 2\alpha \sin 2\beta| = 1$ . This corresponds to the situation where the photonic parts of both terms in Eq. (2) are projected on a common state with equal amplitude. The amplitude of the quantum term is partially governed by the ratio  $v/h = (|v|/|h|)e^{i(\Delta\phi + \Delta\phi_c)}$ , which includes all perturbations inherent to the setup that affect the balance between the horizontal polarization and the vertical polarization. Finally, the magnitude of quantum interference is also determined by the overlap between different environment states  $\langle E_V|E_H \rangle = |\langle E_V|E_H \rangle| e^{i\Delta\phi_E}$ , which represents quantum mechanical decoherence. The presence of  $\Delta\phi_c$  in the last cosine factor of the quantum interference term shows that to make judgments about quantum decoherence, one has to take great care in eliminating or measuring phase differences between different polarizations. This can be done by inserting another birefringent element in the setup that will compensate the phase difference between the two polarizations. Optimization and alignment of our SPDC source includes tweaking of a  $\lambda/4$  plate (Fig. 1), which allows us to experimentally eliminate  $\Delta\phi_c$  in Eq. (3).

We now consider  $h = v$ , which represents equal probability of detecting horizontally or vertically polarized pairs of photons and is fulfilled when a circular hole array is used. In the case of perfect coherence  $\langle E_V|E_H \rangle = 1$  ( $E_V = E_H$ ), we get the rather simple expression  $P_{CC}(\alpha, \beta) = \frac{1}{2} \cos^2(\alpha - \beta)$ . There is no entanglement between the photon state and the environment. This ensures the preservation of polarization entanglement between photons. By contrast, in the case of total decoherence  $\langle E_V|E_H \rangle = 0$ , we get a constant probability  $P_{CC}(\alpha, \beta = 45^\circ) = \frac{1}{4}$  regardless of  $\alpha$  (if  $\beta$  is kept fixed at  $45^\circ$ ). Both terms of the superposition in Eq. (2) are now incoherent, and quantum interferences vanish. The measured state can be considered as a statistical mixture of the two states  $|H, H\rangle$  and  $|V, V\rangle$  in equal proportions.

These considerations suggest a measure of quality of the entanglement, visibility, which we define simply as the visibility of the cosine curve described by  $P_{CC}(\alpha, \beta = 45^\circ)$  for the case when we keep polarizer  $\beta$  fixed at  $45^\circ$  (both polarizations contribute to the measurement),  $V = (P_{CC}^{\max} - P_{CC}^{\min}) / (P_{CC}^{\max} + P_{CC}^{\min})$ , where  $P_{CC}^{\min}$  is the minimum probability of coincidence count (rate in an experiment) and  $P_{CC}^{\max}$  is the maximum count rate. For  $h = v$  and  $\Delta\phi_c = 0^\circ$ ,  $V = |\langle E_V|E_H \rangle| \cos \Delta\phi_E$ . From the above analysis we get  $V = 100\%$  for fully entangled (quantum) light ( $\langle E_V|E_H \rangle = 1$ ) and  $V = 0\%$  for a pure statistical mixture

of polarizations (“classical” light,  $\langle E_V|E_H \rangle = 0$ ). Note that visibility of the cosine  $P_{CC}(\alpha, \beta = 45^\circ)$  is identical to the visibility of the cosine  $P_{CC}(\alpha, \beta = 135^\circ)$ , and hence we can use either one of them, or we can use one versus the other to validate the correctness of the measurement.

In addition, we perform measurements of violation of Bell’s inequalities, where we use Bell’s inequalities in so-called CHSH form [24,25]. We perform 16-point measurements to calculate Bell’s parameter  $S$ , comparing our experimental measurement with the best possible prediction of any classical local hidden-variable theory.  $S > 2$  indicates the impossibility of the explanation by any local hidden-variable theory.

We characterize our SPDC source (Fig. 2) without plasmonic samples, measuring visibility on the order of  $(99 \pm 1)\%$  and  $S = 2.81 \pm 0.02$ , which is just a standard deviation away from the maximal theoretical value  $S_{\max} = 2\sqrt{2} \approx 2.83$ . From this, we conclude that we have high-quality pairs of entangled photons. In the next section, we investigate the influence of the insertion of a plasmonic hole array on the quality of entanglement between photons, as defined by the previous measurement procedures.

## B. Hole array with nonlinear dispersion

In this section, we investigate the same polarization-entanglement process using this time single SPPs that propagate in a hole array, and most importantly in a regime of highly nonlinear dispersion, far from the light line, in an attempt to reveal effects of pure dephasing on decoherence through a decrease of entanglement visibility. In the highly dispersive regime, the quasiparticle confinement at the metal-dielectric interface is much stronger due to the

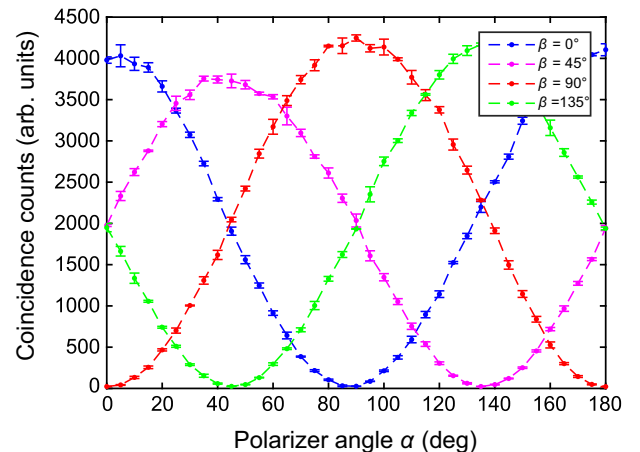


FIG. 2. Calibration of the setup, and entanglement between produced pairs of photons. Number of coincidence counts as a function of polarizer angles without a plasmonic sample (solid lines are fits to a cosine function). The visibility of the different cosine fits is nearly equal to 1, indicating quasiperfect entanglement between the photons of our SPDC source.



reduction in the plasmon wavelength. In other words, the plasmon excitation wave function has a much larger overlap with the electronic degrees of freedom in the metal. As a consequence, plasmons in the highly dispersive regime generally have a higher rate of interaction with the electronic system than in the case of materials with linear dispersion. Hence, in addition to a shorter total decoherence time  $T_2$ , one can expect a shorter pure dephasing time  $T_2^*$  (which is the relevant timescale probed by our experiment). The group velocity of highly dispersive plasmons can be an order of magnitude smaller than for plasmons in the “photonlike” regime, so these plasmons propagate for a longer time  $t_p$  (even if the propagation distances are the same). Therefore, for comparable experiments (i.e., similar propagation distances), strongly confined plasmons are expected to experience greater decoherence and thus exhibit weaker quantum interference than photonlike plasmons.

As a warm-up experiment and to be able to compare the influence of the nonlinearity of the dispersion regime with that of the linear regime, we perform a series of experiments with hole arrays and plasmons propagating at the gold-glass interface, the structure being optimized to operate in the linear (“photonlike”) dispersion regime. The results are shown in Supplemental Material [26]; we find no evidence of decoherence when close to the light line, as was frequently reported until now.

To probe the highly dispersive regime in an analogous situation, we excite plasmons at the interface between gold and amorphous silicon. Amorphous silicon has a higher dielectric constant than glass, moving the surface plasma frequency close to the frequency of entangled photons (see Fig. 3). The use of a higher-index material leads both to stronger SPP confinement and significantly enhanced light-matter interaction compared with plasmons propagating at the interface between gold and glass (in the “photonlike” regime): a sixfold increase of the plasmon wave vector, a 12-fold reduction of the group velocity ( $0.05c$  versus  $0.59c$ , where  $c$  is the speed of light in a vacuum), and more than 100-fold reduction in the absorption length ( $200\text{ nm}$  vs  $27\text{ }\mu\text{m}$ ).

By performing finite-difference time-domain simulations with Lumerical FDTD software, we obtain transmission spectra of a variety of nanohole-array structures with different geometries and periodicities. The positions of the transmission maxima are considered as indicative of the resonance energies and of the dispersion relation of the surface plasmons. An initial choice for the range of geometrical parameters (hole dimensions, array periodicity, films thicknesses) in our experiment is made using the parameters of the simulated structures that exhibited enhanced extraordinary optical transmission at  $812\text{ nm}$ —the wavelength of our down-converted photons.

Subsequently, we fabricate a number of hole arrays with different geometrical parameters within this range to

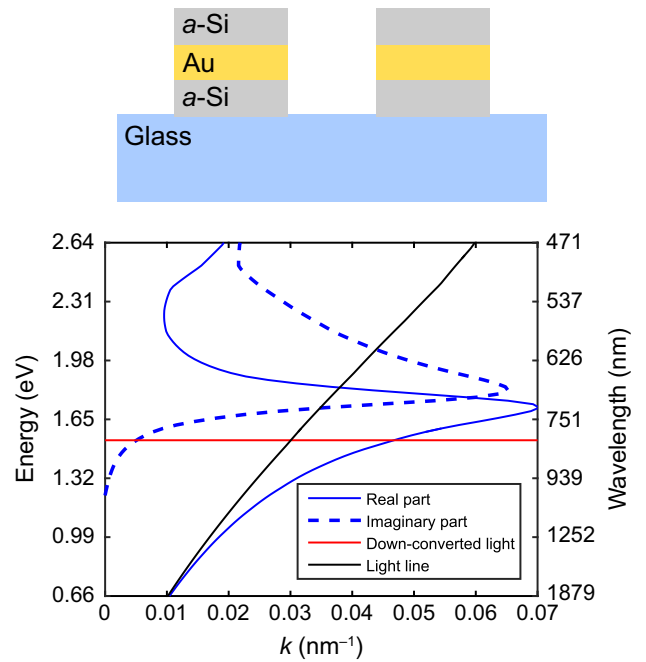


FIG. 3. Plasmonic-hole-array design in our experiment: cross-section schematic (top) and dispersion relation of circular hole arrays for SPPs supported in the silicon-gold-silicon structure, which exhibits strongly nonlinear dispersion at  $812\text{ nm}$  (bottom). The red line shows the energy of the plasmons excited in our experiment.

experimentally find the structure that achieves the target performance. This procedure allows us to identify and fabricate a sample with optimal design, which is a  $2 \times 2\text{ mm}^2$  hole array configured in a three-layer structure ( $50\text{ nm}$  of amorphous silicon,  $100\text{ nm}$  of gold, and  $50\text{ nm}$  of amorphous silicon) and with periodicity  $P = 850\text{ nm}$  [Fig. 4(a)]. We find a plasmon-enhanced transmission peak at the desired wavelength of  $812\text{ nm}$  [Fig. 4(b)]. In this hole array, SPPs excited on the top and bottom gold surfaces are uncoupled and have the same dispersion. We perform additional analysis and confirm that the fabricated structure correctly reproduces the initially simulated behavior and operates in the nonlinear-dispersion regime, far from the light line [27].

Because of the rather large size of the sample we were able to collect a large portion of transmitted light and hence improve our statistics, even in the presence of considerable losses and with intrinsically low transmission [Fig. 4(c)]. We recorded a visibility  $V$  of  $(98 \pm 2)\%$  and Bell’s number  $S = 2.83 \pm 0.04$ : this measurement implies that even in the highly dispersive regime, the entanglement is perfectly preserved and no quantitative signs of pure dephasing could be detected. Through numerical computation of the dispersion relation, we can estimate the propagation time  $t_p$  to be on the order of approximately  $1.2\text{ }\mu\text{m}/0.05c \sim 80\text{ fs}$ , on the basis of the distance between

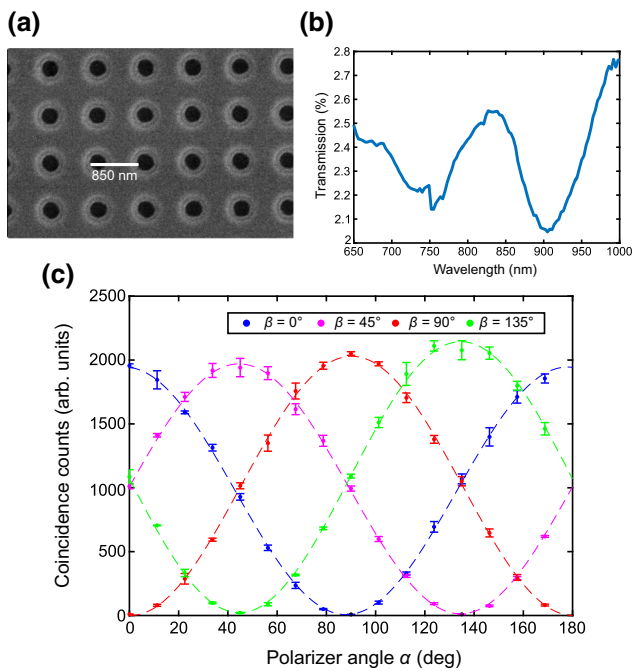


FIG. 4. Hole array for plasmons in the highly dispersive regime. (a) SEM image of the sample. The period of the two-dimensional array is 850 nm. The different material species experience a different milling rate, which slightly affects the shape of the hole perimeter. (b) Transmission spectrum of the hole array. Because the holes are circular, there is no polarization dependence. The broadening of the transmission feature around 810 nm can be attributed to the imperfect shape of the holes. The plasmons experience significant absorption. (c) Coincidence counts as a function of polarizer angles in the presence of the hole array with a highly dispersive regime (solid lines are fits to a cosine function). Whatever the choice of  $\beta$ , and even when  $\beta$  is  $4^\circ$  or  $135^\circ$ , the visibility of quantum interference remains almost equal to 1, indicating near-perfect preservation of entanglement between particles.

two diagonally separated holes (this is the relevant distance in our case, since eigenmodes of our hole array are diagonally oriented, similarly to the case in Ref. [16]). This time is much longer than the literature-reported value ([19,28]) of the SPP total dephasing time  $T_2 = 20\text{--}30$  fs (in agreement with our own estimations from either simulated or experimental data). This confirms the fact discussed above that in our experiment the relevant decoherence mechanism is pure dephasing, caused by elastic scattering of SPPs, rather than dephasing due to inelastic scattering (i.e., population decay). Since in our experiment we measure visibility to be almost 100% (within the margin of experimental precision), we conclude that in our system pure dephasing is a remarkably slow process compared with absorption and the SPP pure dephasing time  $T_2^*$  must be much longer than the propagation time, and we put a conservative order-of-magnitude estimate of 100 fs on

its lower bound, which is similar to the value reported in Ref. [19].

However, this time could be in practice much longer, as our experiment remarkably reports no quantitative trace of quantum decoherence. Performing the same experiment in an even more highly dispersive regime could hypothetically allow us to make the decoherence process eventually visible to some extent. This would make the degradation of the visibility of fringes capable of being modeled, one of the parameters of such a model being the pure dephasing time, which could be more-precisely estimated. The design of such an experiment is, however, fundamentally, limited by the high level of absorption that coexists with the enhancement of light-matter interactions. It dramatically reduces the signal level at the output of the plasmonic path progressively to almost zero.

In summary, we examine the influence of plasmon dispersion on the quantum decoherence properties of surface plasmons. The excitation of highly dispersive plasmons does not result in the reduction of the quality of a single-particle quantum state for transmitted light. Plasmons excited in hole arrays are found to preserve quantum mechanical correlations, even in the presence of extreme dispersion near the plasmon resonance and strong absorption. Moreover, the focus of our measurements is on the elastic dephasing processes, the consideration of which is commonly neglected in quantum optics modeling due to its supposed insignificance. Our findings provide experimental proof for such an assumption, and also emphasize the difference between decay and decoherence. Thus, we conclude that despite being lossy, plasmonic structures may find applications in the realms of quantum technology, where the power of extreme light confinement can be effectively leveraged.

### Acknowledgments

We acknowledge Yousif Kelaita, Artur Davoyan, Ruzan Sokhoyan, Ragip Pala, Dagny Fleischman, Zachary Aitken, and Sunita Darbe for help with equipment training and scientific advice. This work was supported by the Air Force Office of Scientific Research under Grant No. FA9550-16-1-0019.

Y.S.T., J.S.F., and H.A.A. proposed the original idea. Y.S.T. realized all experiments and data analysis. B.V. helped in discussion. Y.S.T., B.V., and H.A.A. wrote the paper, and all authors discussed and revised the manuscript.

- [1] E. Knill, R. Laflamme, and G. J. Milburn, A scheme for efficient quantum computation with linear optics, *Nature* **409**, 46 (2001).

- [2] J. Sun, E. Timurdogan, A. Yaacobi, E. S. Hosseini, and M. R. Watts, Large-scale nanophotonic phased array, *Nature* **493**, 195 (2013).
- [3] R. H. Ritchie, Plasma losses by fast electrons in thin films, *Phys. Rev.* **106**, 874 (1957).
- [4] R. Alvarez-Puebla, J. P. B.-V. B. Cui, T. Veres, and H. Fenniri, Nanoimprinted sers-active substrates with tunable surface plasmon resonances, *J. Phys. Chem. C* **111**, 6720 (2007).
- [5] J. Homola, Surface plasmon resonance sensors for detection of chemical and biological species, *Chem. Rev.* **108**, 462 (2008).
- [6] M. Tabatabaei, M. Najiminaini, K. Davieau, B. Kaminaska, M. R. Singh, J. J. L. Carson, and F. Lagugné-Labarhet, Tunable 3d plasmonic cavity nanosensors for surface-enhanced raman spectroscopy with sub-femtomolar limit of detection, *ACS Photonics* **2**, 752 (2015).
- [7] T. Taubner, D. Korobkin, Y. Urzhumov, G. Shvets, and R. Hillenbrand, Near-field microscopy through a sic superlens, *Science* **313**, 1595 (2006).
- [8] J. N. Farahani, D. W. Pohl, H.-J. Eisler, and B. Hecht, Single Quantum dot Coupled to a Scanning Optical Antenna: A Tunable Superemitter, *Phys. Rev. Lett.* **95**, 17402 (2005).
- [9] J. Dintinger, S. Klein, F. Bustos, W. L. Barnes, and T. W. Ebbesen, Strong coupling between surface plasmon-polaritons and organic molecules in subwavelength hole arrays, *Phys. Rev. B* **71**, 035424 (2005).
- [10] D. E. Chang, A. S. Sorensen, P. R. Hemmer, and M. D. Lukin, Strong coupling of single emitters to surface plasmons, *Phys. Rev. B* **76**, 035420 (2007).
- [11] M.-C. Dheur, E. Devaux, T. W. Ebbesen, A. Baron, J.-C. Rodier, J.-P. Hugonin, J.-J. Greffet, G. Messin, and F. Marquier, Single-plasmon interferences, *Sci. Adv.* **2**, e1501574 (2016).
- [12] R. Kolesov, B. Grotz, G. Balasubramanian, R. J. Stöhr, A. A. Nicolet, P. R. Hemmer, F. Jelezko, and J. Wrachtrup, Wave-particle duality of single surface plasmon polaritons, *Nat. Phys.* **5**, 470 (2009).
- [13] J. S. Fakonas, H. Lee, Y. A. Kelaita, and H. A. Atwater, Two-plasmon quantum interference, *Nat. Photonics* **8**, 317 (2014).
- [14] G. D. Martino, Y. Sonnefraud, M. Tame, S. Kéna-Cohen, F. Dieleman, Ş. K. Özdemir, M. S. Kim, and S. A. Maier, Observation of Quantum Interference in the Plasmonic Hong-ou-mandel Effect, *Phys. Rev. Appl.* **1**, 034004 (2014).
- [15] B. Vest, M.-C. Dheur, É. Devaux, A. Baron, E. Rousseau, J.-P. Hugonin, J.-J. Greffet, G. Messin, and F. Marquier, Anti-coalescence of bosons on a lossy beam splitter, *Science* **356**, 1373 (2017).
- [16] E. Altewischer, M. P. Exter, and J. P. Woerdman, Plasmon-assisted transmission of entangled photons, *Nature* **418**, 304 (2002).
- [17] M.-C. Dheur, B. Vest, É. Devaux, A. Baron, J.-P. Hugonin, J.-J. Greffet, G. Messin, and F. Marquier, Remote preparation of single-plasmon states, *Phys. Rev. B* **96**, 045432 (2017).
- [18] J. S. Fakonas, A. Mitskovets, and H. A. Atwater, Path-entanglement of surface plasmons, *New J. Phys.* **17**, 023002 (2015).
- [19] S. G. Dlamini, J. T. Francis, X. Zhang, Ş. K. Özdemir, S. N. Chormaic, F. Petruccione, and M. S. Tame, Probing Decoherence in Plasmonic Waveguides in the Quantum Regime, *Phys. Rev. Appl.* **9**, 024003 (2018).
- [20] T. W. Ebbesen, H. J. Lezec, H. F. Ghaemi, T. Thio, and P. A. Wolff, Extraordinary optical transmission through sub-wavelength hole arrays, *Nature* **391**, 667 (1998).
- [21] S. Balakrishnan, M. Najiminaini, M. R. Singh, and J. J. L. Carson, A study of angle dependent surface plasmon polaritons in nano-hole array structures, *J. Appl. Phys.* **120**, 034302 (2016).
- [22] M. R. Singh, M. Najiminaini, S. Balakrishnan, and J. J. L. Carson, Metamaterial-based theoretical description of light scattering by metallic nano-hole array structures, *J. Appl. Phys.* **117**, 184302 (2015).
- [23] R. Rangarajan, M. Goggin, and P. Kwiat, Optimizing type-I polarization-entangled photons, *Opt. Express* **17**, 18920 (2009).
- [24] J. Bell, On the problem of hidden variables in quantum mechanics, *Rev. Mod. Phys.* **38**, 447 (1966).
- [25] J. Clauser, M. Horne, A. Shimony, and R. Holt, Proposed Experiment to Test Local Hidden-variable Theories, *Phys. Rev. Lett.* **23**, 880 (1969).
- [26] See Supplemental Material at <http://link.aps.org/supplemental/10.1103/PhysRevApplied.12.044037> for discussions on experiments performed in the linear regime.
- [27] See Supplemental Material at <http://link.aps.org/supplemental/10.1103/PhysRevApplied.12.044037> for discussions on the operation of the hole-array structure in the highly dispersive regime.
- [28] K. Puech, F. Z. Henari, W. J. Blau, D. Duff, and G. Schmid, Investigation of the ultrafast dephasing time of gold nanoparticles using incoherent light, *Chem. Phys. Lett.* **247**, 13 (1995).